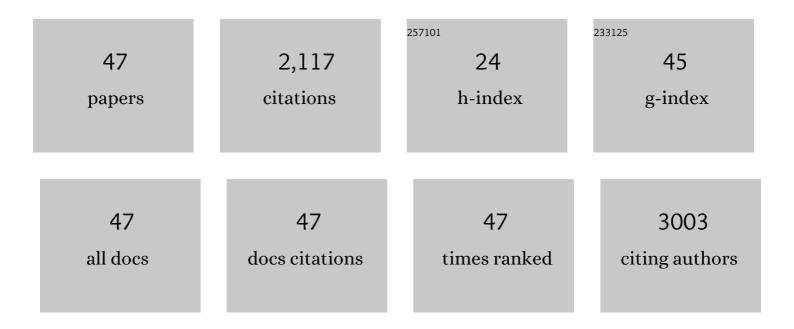
Zhonghua Li

List of Publications by Year in descending order

Source: https://exaly.com/author-pdf/7701070/publications.pdf Version: 2024-02-01



#	Article	IF	CITATIONS
1	High-responsivity photodetector based on scrolling monolayer MoS ₂ hybridized with carbon quantum dots. Nanotechnology, 2022, 33, 105301.	1.3	10
2	Engineering the Optoelectronic Properties of 2D Hexagonal Boron Nitride Monolayer Films by Sulfur Substitutional Doping. ACS Applied Materials & Interfaces, 2022, 14, 16453-16461.	4.0	10
3	Terminal p-ï€ conjugation induced excited-state symmetry-breaking charge separation for porous carbon nitride based heterojunction. Journal of Alloys and Compounds, 2021, 882, 160550.	2.8	7
4	Improved Interface Charge Transfer and Redistribution in CuOâ€CoOOH pâ€n Heterojunction Nanoarray Electrocatalyst for Enhanced Oxygen Evolution Reaction. Advanced Science, 2021, 8, e2103314.	5.6	100
5	Black reduced porous SnO2 nanosheets for CO2 electroreduction with high formate selectivity and low overpotential. Applied Catalysis B: Environmental, 2020, 260, 118134.	10.8	107
6	Mesocrystalline Ta3N5 superstructures with long-lived charges for improved visible light photocatalytic hydrogen production. Journal of Colloid and Interface Science, 2020, 560, 359-368.	5.0	58
7	The role of hybrid dielectric interfaces in improving the performance of multilayer InSe transistors. Journal of Materials Chemistry C, 2020, 8, 6701-6709.	2.7	8
8	Visible light photocatalysis of amorphous Cl-Ta2O5â^'x microspheres for stabilized hydrogen generation. Journal of Colloid and Interface Science, 2020, 572, 141-150.	5.0	62
9	A crystalline–amorphous Ni–Ni(OH) ₂ core–shell catalyst for the alkaline hydrogen evolution reaction. Journal of Materials Chemistry A, 2020, 8, 23323-23329.	5.2	77
10	Understanding the Phase-Induced Electrocatalytic Oxygen Evolution Reaction Activity on FeOOH Nanostructures. ACS Catalysis, 2019, 9, 10705-10711.	5.5	233
11	Boosting visible light photocatalytic activity via impregnation-induced RhB-sensitized MIL-125(Ti). Chemical Engineering Research and Design, 2019, 143, 90-99.	2.7	49
12	One-step synthesis of oxygen vacancy-rich SnO2 quantum dots with ultrahigh visible-light photocatalytic activity. Materials Research Bulletin, 2019, 118, 110486.	2.7	16
13	Mesocrystalline Ta2O5 nanosheets supported Pd Pt nanoparticles for efficient photocatalytic hydrogen production. International Journal of Hydrogen Energy, 2018, 43, 8232-8242.	3.8	22
14	Construction of hybrid Ag2CO3/AgVO3 nanowires with enhanced visible light photocatalytic activity. Materials Research Bulletin, 2018, 101, 246-252.	2.7	23
15	Bimetal-organic frameworks derived carbon doped ZnO/Co 3 O 4 heterojunction as visible-light stabilized photocatalysts. Materials Science in Semiconductor Processing, 2018, 79, 24-31.	1.9	20
16	Superstructure Ta ₂ O ₅ mesocrystals derived from (NH ₄) ₂ Ta ₂ O ₃ F ₆ mesocrystals with efficient photocatalytic activity. Dalton Transactions, 2018, 47, 1948-1957.	1.6	21
17	Facile synthesis of Ti 3+ -TiO 2 mesocrystals for efficient visible-light photocatalysis. Journal of Physics and Chemistry of Solids, 2018, 119, 94-99.	1.9	15
18	Plasmon-resonance-enhanced visible-light photocatalytic activity of Ag quantum dots/TiO 2 microspheres for methyl orange degradation. Solid State Sciences, 2018, 80, 1-5.	1.5	17

Zhonghua Li

#	Article	IF	CITATIONS
19	Mesocrystalline Ti3+TiO2 hybridized g-C3N4 for efficient visible-light photocatalysis. Carbon, 2018, 128, 21-30.	5.4	110
20	Synthesis of <i>β</i> -AgVO ₃ nanowires decorated with Ag ₂ CrO ₄ , with improved visible light photocatalytic performance. Semiconductor Science and Technology, 2018, 33, 055010.	1.0	9
21	Synthesis of mixâ€faceted Cu ₂ O nanoparticles with tunable {111} and {100} facet ratios for enhanced photocatalytic activity. Micro and Nano Letters, 2018, 13, 135-137.	0.6	4
22	One-step synthesis of the single crystal Ta2O5 nanowires with superior hydrogen production activity. Materials Letters, 2017, 191, 150-153.	1.3	17
23	Defect engineered Ta2O5 nanorod: One-pot synthesis, visible-light driven hydrogen generation and mechanism. Applied Catalysis B: Environmental, 2017, 217, 48-56.	10.8	84
24	Facile synthesis of Ti 3+ doped Ag/AgI TiO 2 nanoparticles with efficient visible-light photocatalytic activity. International Journal of Hydrogen Energy, 2017, 42, 13031-13038.	3.8	21
25	Facile synthesis of Ag ₃ VO ₄ /β-AgVO ₃ nanowires with efficient visible-light photocatalytic activity. RSC Advances, 2017, 7, 27515-27521.	1.7	49
26	Non-planar vertical photodetectors based on free standing two-dimensional SnS ₂ nanosheets. Nanoscale, 2017, 9, 9167-9174.	2.8	57
27	Ta O C chemical bond enhancing charge separation between Ta4+ doped Ta2O5 quantum dots and cotton-like g-C3N4. Applied Catalysis B: Environmental, 2017, 205, 271-280.	10.8	73
28	Efficiently Synergistic Hydrogen Evolution Realized by Trace Amount of Pt-Decorated Defect-Rich SnS ₂ Nanosheets. ACS Applied Materials & Interfaces, 2017, 9, 37750-37759.	4.0	76
29	PCR-Free Colorimetric DNA Hybridization Detection Using a 3D DNA Nanostructured Reporter Probe. ACS Applied Materials & Interfaces, 2017, 9, 38281-38287.	4.0	28
30	Synthesis of plasmonic Ti ³⁺ doped Au/Cl-TiO ₂ mesocrystals with enhanced visible light photocatalytic activity. Dalton Transactions, 2017, 46, 11898-11904.	1.6	19
31	Synthesis of Ti3+ and P5+ co-doped TiO2 nanocrystal with enhanced visible light photocatalytic activity. Catalysis Communications, 2017, 102, 1-4.	1.6	11
32	Vertically aligned two-dimensional SnS ₂ nanosheets with a strong photon capturing capability for efficient photoelectrochemical water splitting. Journal of Materials Chemistry A, 2017, 5, 1989-1995.	5.2	117
33	Heterostructured Ag3PO4/TiO2 film with high efficiency for degradation of methyl orange under visible light. Thin Solid Films, 2014, 551, 8-12.	0.8	21
34	Photocatalytic hydrogen production over In2S3–Pt–Na2Ti3O7 nanotube films under visible light irradiation. Ceramics International, 2013, 39, 8059-8063.	2.3	12
35	Preparation and photocatalytic activity for water splitting of Pt–Na2Ta2O6 nanotube arrays. Journal of Solid State Chemistry, 2013, 198, 192-196.	1.4	15
36	Effect of Pt loading and calcination temperature on the photocatalytic hydrogen production activity of TiO2 microspheres. Ceramics International, 2013, 39, 5387-5391.	2.3	56

Zhonghua Li

#	Article	IF	CITATIONS
37	Single crystal titanate–zirconate nanoleaf: Synthesis, growth mechanism and enhanced photocatalytic hydrogen evolution properties. CrystEngComm, 2012, 14, 1874.	1.3	15
38	Template free synthesis of crystallized nanoporous F-Ta2O5 spheres for effective photocatalytic hydrogen production. Nanoscale, 2012, 4, 3867.	2.8	24
39	Ag loaded flower-like BaTiO ₃ nanotube arrays: Fabrication and enhanced photocatalytic property. CrystEngComm, 2012, 14, 1473-1478.	1.3	74
40	Cu2O/Cu/TiO2 nanotube Ohmic heterojunction arrays with enhanced photocatalytic hydrogen production activity. International Journal of Hydrogen Energy, 2012, 37, 6431-6437.	3.8	140
41	Photocatalytic hydrogen production from water/methanol solutions over highly ordered Ag–SrTiO3 nanotube arrays. International Journal of Hydrogen Energy, 2011, 36, 5811-5816.	3.8	41
42	Design of highly ordered Ag–SrTiO3 nanotube arrays for photocatalytic degradation of methyl orange. Journal of Solid State Chemistry, 2011, 184, 1924-1930.	1.4	29
43	A facile template-free method for preparing bi-phase TiO2 nanowire arrays with high photocatalytic activity. Materials Letters, 2010, 64, 1776-1778.	1.3	18
44	Effects of calcination temperature on the morphology, structure and photocatalytic activity of titanate nanotube thin films. Thin Solid Films, 2010, 519, 541-548.	0.8	32
45	Photocatalytic Water Splitting Over a Protonated Layered Perovskite Tantalate H1.81Sr0.81Bi0.19Ta2O7. Catalysis Letters, 2008, 123, 80-83.	1.4	31
46	Photocatalytic property of La2Ti2O7 synthesized by the mineralization polymerizable complex method. Materials Research Bulletin, 2008, 43, 1781-1788.	2.7	31
47	One-Step Controllable Synthesis for High-Quality Ultrafine Metal Oxide Semiconductor Nanocrystals via a Separated Two-Phase Hydrolysis Reaction. Journal of the American Chemical Society, 2008, 130, 2676-2680.	6.6	48